Title
DETERMINATION OF PHASE DIAGRAMS USING DIFFUSION TECHNIQUES

Authors
Pask, Joseph A.
Aksay, Ilhan A.

Publication Date
1974-08-01

Presented at the Conference on Ceramic
Science Transport Phenomena in Ceramics,
Case Western Reserve University, Cleveland,
Ohio, June 3 - 5, 1974

LBL-2599

DETERMINATION OF PHASE DIAGRAMS USING DIFFUSION TECHNIQUES

Joseph A. Pask and Ilhan A. Aksay

August, 1974

Prepared for the U. S. Atomic Energy Commission
under Contract W-7405-ENG-48

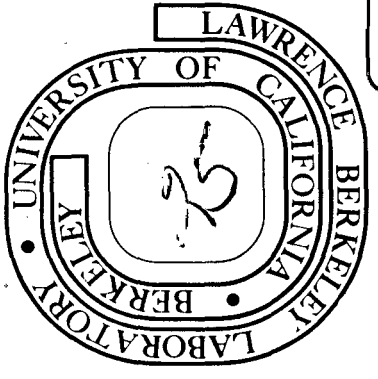

LBL-2599

DISCLAIMER

DETERMINATION OF PHASE DIAGRAMS USING DIFFUSION TECHNIQUES

Joseph A. Pask and Ilhan A. Aksay

August 1974

DETERMINATION OF PHASE DIAGRAMS USING DIFFUSION TECHNIQUES

Joseph A. Pask

Inorganic Materials Research Division, Lawrence Berkeley Laboratory

and Department of Materials Science and Engineering,

College of Engineering; University of California,

Berkeley, California 94720

and

Ilhan A. Aksay

Xerox Corporation

Webster Research Center

Webster, New York 14580

ABSTRACT

Semi-infinite diffusion couple arrangements between two condensed phases can be readily analyzed with the use of the electron beam microprobe analyzer to determine the composition profiles in the two end phases of the couple arrangement and in any intermediate phases that may grow between the end phases. When the reactions at the interfaces are diffusion controlled, chemical equilibrium exists at each interface and each interfacial composition then corresponds to either a liquidus or a solidus composition, and these interfacial compositions, with the aid of microstructural observations, can be used in the construction of the stable and/or metastable equilibrium phase diagrams involving the end phases of the diffusion couple. This technique is applied to the study of phase equilibria in the SiO_2-Al_2O_3 system.

1. INTRODUCTION

Techniques of phase equilibrium studies may be grouped into two general categories: (i) static techniques, and (ii) dynamic techniques. In static techniques a specimen is held at a fixed point in pressure-temperature-composition space until equilibrium is achieved and subsequently analyzed to determine its equilibrium phase assemblage. The most commonly used analysis technique is based on microstructural observations of a representative cross-section after such a sample is quenched to room temperature. Dynamic techniques, on the other hand, are based on the measurement of anomalies in a physico-chemical property during phase transformations as one of the variables in the P-T-x space is continuously changed. Various techniques of both categories have been reviewed extensively.[1,2] In systems where stable equilibrium conditions are not easily attained, as in silicates, obtaining accurate phase equilibrium data by only one single technique is quite different. It is generally agreed that combination of several techniques may be utilized to decipher the stable phase equilibrium of a system which is complicated by the existence of metastable conditions.

The diffusion couple technique, although not widely utilized, is unique since it combines certain features of the static and dynamic techniques into a single experiment. The purpose of this paper is to discuss the principles of this technique and illustrate its utility in the study of phase equilibrium in the SiO_2-Al_2O_3 system.

2. DIFFUSION COUPLE TECHNIQUE

When two phases of a binary system that are not at thermodynamic equilibrium with each other are brought into contact and annealed at a sufficiently high temperature, atom mobility is enhanced, and the components of these end phases interdiffuse to achieve a state of chemical equilibrium. The diffusion

of the components is in such a direction as to eliminate any chemical potential gradient. At constant T and P, under equilibrium conditions, all the phase fields intersected by the corresponding isotherm and the isobar between the end phases will form as layers in the diffusion zone. The thickness of each layer is dependent upon the growth rate of the corresponding phase.[3-6] Regardless of its thickness, however, each phase must exist in the diffusion zone in order to provide a continuous and monotonic chemical potential gradient throughout the zone. If diffusion transport is the rate controlling mechanism, a local chemical equilibrium will exist at each interface, and the motion of each interface will be proportional to the square root of annealing time.[3] These interfacial compositions, then, correspond to either a liquidus or a solidus composition[7] and can be used to construct the equilibrium phase diagram involving the end phases of the diffusion couple.

In a binary system, when a diffusion couple is annealed until the entire system attains equilibrium, a maximum of only two phases and one interface will remain if the overall composition of the couple corresponds to a two-phase region or only one phase if the overall composition corresponds to a solution field. At this stage, the couple loses its significance since it then provides only the information that one would obtain from a single specimen treated by the static method of quenching. At intermediate stages (Figs. 1 and 2), when the couple still retains its semi-infinite features, the phase rule is satisfied only locally at each point. The couple then resembles an ensemble of specimens subjected to the static method of quenching along the entire system. The examination of a single diffusion profile, at a temperature, provides all the information needed for the system at that isotherm.

In a ternary system, the appearance of a continuous interface in a diffusion couple represents an invariant region as represented by the three-phase

($\alpha + \beta$ + Liquid) region of the system shown in Fig. 3.[8] Two-phase regions appear as a band with the compositions of the corresponding phases varying along the band as dictated by the tie-lines. A couple between the end compositions of X and B (Fig. 3) will contain two such bands corresponding to the $\alpha + L$ and $\alpha + \beta$ regions. The compositions of the α and L phases in the first band will vary from α_f and L_f to α_c and L_c towards the $L + \alpha + \beta$ interface. Similarly, the compositions of the α and β phases in the second band will vary from α_a and β_a to α_c and β_c towards the $L + \alpha + \beta$ interface. In the single-phase layers of α and β, the composition profiles will vary from X to α_f and B to β_a, assuming that composition path coincides with the line XB.

Although the advantages of the diffusion couple technique were discussed in the 50's,[8-10] without the availability of the electron beam microprobe analysis, its application was limited. During the last decade, however, with the aid of the electron beam microprobe techniques, this method has been applied to the study of phase equilibrium in various metallic[11] and ceramic[12] systems. A most recent application[13,14] of this technique to a basic ceramic system is summarized in the next section.

3. THE SiO_2-Al_2O_3 SYSTEM

Since the classic work of Bowen and Greig,[15] in 1924, phase equilibrium in the SiO_2-Al_2O_3 system has been studied extensively.[16] The results of these numerous studies have conflicted mainly on two issues: (i) the melting behavior, and (ii) the extent of the solid solution range of the intermediate compound of the system, mullite ($3Al_2O_3 \cdot 2SiO_2$). These conflicting results have been the result of incomplete information obtained from the static method of quenching or differential thermal analysis techniques used in most of these studies. Among these, the studies by Trömel et al.[17] and Aramaki and Roy[18] were the most extensive and representative. The findings of Trömel et al., in

general, are in agreement with those of Bowen and Greig which indicate an incongruent melting behavior of mullite. On the other hand, Aramaki and Roy indicate a congruent melting point for mullite.

Similarly, the stable solid solution range of mullite has been reported to extend from 71.8 wt% to ≈74.3 wt% Al_2O_3.[18] This range, however, was only realized when mullite was prepared by solid state reactions in the presence of alumina. When solidified from a melt, the composition of mullite may extend up to 82.6 wt% Al_2O_3[19] raising the question of metastability and the possible existence of a disordered form of mullite with a nominal composition of $2Al_2O_3 \cdot SiO_2$.[18] Recently, the diffusion couple technique, combined with microstructural observations, has been most useful in providing a unified explanation to these conflicting observations on the phase equilibrium in the SiO_2-Al_2O_3 system.[13,14]

The equilibrium SiO_2-Al_2O_3 phase diagram based on the information obtained from electron beam microprobe analysis of semi-infinite diffusion couples of fused silica-sapphire is shown in Fig. 4. The data points which correspond to the interfacial compositions along the concentration profiles (Fig. 4) are the equilibrium compositions since they remained constant with annealing time and since the transport process was shown to be diffusion controlled.[13,14] These interfacial compositions, then, clearly outline the stable equilibrium diagram as shown with solid lines in Fig. 4. Here the possibility of the equilibrium of alumina or mullite with a metastable liquid is overruled since it is unlikely to have more than one free energy of mixing-composition relationship for the liquid phase and thus there can be only one equilibrium state between alumina or mullite and the liquid phase. The most important feature of this diagram is that it indicates an incongruent melting for mullite at 1828°C and outlines a maximum solid solution range of 70.5 to 74.0 wt% Al_2O_3

under stable equilibrium conditions.

This incongruent melting behavior of mullite and its solid solution range, however, are not easily verified when static method of quenching or dynamic phase equilibrium experiments are performed.[14] Due to metastable existence of a silica-mullite equilibrium in the absence of alumina, as shown with broken lines in Fig. 4, mullite can be superheated above its stable incongruent melting temperature and show a metastable congruent melting behavior at ≈1890°C. This metastability also requires an overall extension of the mullite solid solution field to compositions (≈83.2 wt% Al_2O_3) higher than the stable limit of 74.0 wt% Al_2O_3 as determined in diffusion couple experiments.[14] This super-heating phenomenon, which does not in any way affect the results of the diffusion couple experiments, has been one of two major problems encountered in previous investigations that relied only on static method of quenching or dynamic phase equilibrium experiments.[16]

A second major problem is the supercooling of aluminum silicate liquids, again, a phenomenon which does not affect the results of the diffusion couple experiments but drastically influences the interpretation of microstructures obtained by the static method of quenching. The direct evidences for the supercooling of the aluminum silicate liquids are clearly brought out in the diffusion zone microstructures of three diffusion couples, Fig. 5, each of which was annealed at 1903°C for 15 min but cooled at relatively different rates. These microstructures differ drastically although the average diffusion profiles, and the liquidus compositions at the sapphire interface obtained by scanning the electron beam over an area affected by localized crystallization, are identical. The precipitated crystalline phase as determined by electron microprobe and X-ray diffusion is only mullite in the couple that was quenched (Fig. 5A), only alumina in the couple that was cooled

relatively slowly (Fig. 5C), and alumina and mullite in the couple that was cooled at a moderate rate (Fig. 5B). Since the liquidus composition at the peritectic temperature is 52.3 wt% Al_2O_3, $\tilde{\sim}$350 μm of the diffusion zone adjacent to the sapphire would experience some alumina precipitation during an equilibrium cooling (Fig. 4). The absence of alumina in this portion of the diffusion zone of a quenched couple (Fig. 5A) and presence of alumina in a slowly cooled couple (Fig. 5C) can only be explained on the basis of supercooling phenomena of the liquid. It is, thus, important to note that while the overall composition profiles obtained by averaging over an area are independent of the nature of the microstructure itself and will always provide information on the stable equilibrium conditions, experiments based only on microstructural observations could yield conflicting results depending on the experimental conditions followed.

The precipitation of mullite with high alumina contents only from a melt can now be explained when the stable equilibrium phase diagram of Fig. 4 is viewed with the aid of these two additional facts that (i) in the absence of alumina, a metastable silica-mullite equilibrium exists with mullite displaying congruent melting behavior at a maximum of ≈1890°C and ≈83.2 wt% Al_2O_3, and (ii) aluminum-silicate liquids can be supercooled below the alumina and mullite liquidi with subsequent metastable solidification of mullite instead of the stable alumina phase. With rapid cooling rates, alumina solidification can be eliminated completely as in the microstructure of Fig. 5A. The composition of these mullite precipitates may extend beyond the stable solid solution field as indicated by broken lines in Fig. 4. At moderate cooling rates, precipitation of alumina and then mullite is realized. Microstructures displaying such precipitation as in Fig. 5B have often been misinterpreted as eutectic microstructures and thus led to the erroneous conclusion that a

eutectic existed between mullite and alumina.

Finally, the diffusion zone microstructure of Fig. 5C provides a direct evidence for the existence of a metastable silica-alumina phase equilibrium, without any mullite phase, formed by extensions of the silica and alumina liquidus curves. The total absence of mullite in Fig. 5C indicates a sufficiently slow cooling rate to maintain local equilibrium between the liquid and the alumina precipitates and necessitates the metastable extension of the alumina liquidus below the peritectic temperature.[14] It should be noted, however, that although the cooling rate is slow enough to maintain local equilibrium, the overall diffusion profile of this zone, obtained by the scanning beam technique, is identical to those of microstructures in Fig. 5A and 5B and corresponds to the profile at 1903°C since long range diffusion effects during cooling are negligible.

4. SUMMARY AND CONCLUSIONS

The diffusion couple technique when utilized in conjunction with microstructural studies is useful in determining not only the stable equilibrium but metastable equilibrium conditions as well. The utility of this technique is illustrated in the determination of the stable SiO_2-Al_2O_3 equilibrium phase diagram, in which mullite is shown to melt incongruently as originally determined by Bowen and Greig.[15] The examination of the diffusion zone microstructures supports the incongruency of mullite and also yields additional information on the metastable equilibria caused by the supercooling of the aluminum silicate melts. The conflicting nature of the previous phase equilibrium investigations on the SiO_2-Al_2O_3 system has been associated with the supercooling phenomenon of aluminum silicate liquids and with the existence of metastable silica-mullite equilibria in the absence of alumina.

ACKNOWLEDGMENT

This work was done under the auspices of the United States Atomic Energy Commission.

REFERENCES

1. J. B. MacChesney and P. E. Rosenberg, in "Phase Diagrams, Materials Science and Technology," (Allen M. Alper, ed.) Vol. 1, pp. 113-165, Academic Press, New York (1970).

2. Arnold Reisman, "Phase Equilibria, Basic Principles, Applications, Experimental Techniques," Academic Press, New York (1970).

3. C. Wagner, in "Diffusion in Solids, Liquids and Gases," (W. Jost, author) p. 75, Academic Press, New York (1969).

4. J. S. Kirkaldy, Diffusion in Multicomponent Metallic Systems, III. The Motion of Planar Phase Interfaces, Can. J. Phys. 36, 917-25 (1958).

5. G. V. Kidson, Some Aspects of the Growth of Diffusion Layers in Binary Systems, J. Nucl. Mater. 3, 21-29 (1961).

6. G. B. Gibbs, Diffusion Layer Growth in a Binary System, J. Nucl. Mater. 20, 303-306 (1966).

7. J. E. Dorn, J. T. Gier, L. M. K. Boelter, and N. F. Ward, in "Symposium on Surface Treatment of Metals," pp. 166-77, American Society for Metals, Cleveland (1941).

8. F. N. Rhines, "Phase Diagrams in Metallurgy, Their Development and

Application," pp. 50-52, 107-109, and 156-57, McGraw-Hill Book Co., New York (1956).

9. T. Heumann and P. Lohmann, Über die Diffusion in der β-Phase des Systems Silber-Zink, Z. Elektrochem. 59, 849-60 (1955).

10. T. Heumann and F. Heinemann, Mehrphasendiffusion in System Kupfer-Antimon, Z. Elektrochem. 60, 1160-69 (1956).

11. N. Swindells, The Determination of Equilibrium Diagrams by Electron-Probe Microanalysis, J. Inst. Metals 90, 167-71 (1962); J. I. Goldstein and R. E. Ogilvie, in "Congres International sur é Optique des Rayons X et la Microanalyse," (R. Castaing, et al., eds) 4th, pp. 594-602, Orsay, France (1965); Y. Adda and J. Philibert, in "La Diffusion dans les Solides," p. 618, Presses Universitaires de France, Paris (1966); J. R. Eifert, D. A. Chatfield, G. W. Powell, and J. W. Spretnak, Interface Compositions, Motion, and Lattice Transformations in Multi-phase Diffusion Couples, Trans. AIME 242, 66-71 (1968); T. Nishizawa and A. Chiba, Interface Equilibrium in Diffusion Couples, Nippon Kinzoku Gakkaishi 33, 869-70 (1969); G. N. Ronami and S. M. Kuznetsova, in "Teor. Eksp. Metody Issled. Diagramm Sostoyaniya Metal. Sist., Dokl. Soveshch.,"

(N. V. Ageev, ed.) pp. 172-27, Izd, "Nauka," Moscow, USSR (1969); J. D. Braun, Local Equilibrium and Diffusion in Multiphase Couples, Ph. D. Thesis, The Ohio State University, Columbus (1971); and C. P. Heijwegen and G. D. Rieck, Determination of the Phase Diagram of the Mo-Co System Using Diffusion Couples, J. Less-Common Met. 34 309-14 (1974).

12. J. M. Short and R. Roy, Use of Interdiffusion to Determine Crystalline Solubility in Alkali Halide Systems, J. Am. Ceram. Soc. 47, 149-51 (1964); G. W. Brindley and R. Hayami, Kinetics and Mechanism of Formation of Forsterite (Mg_2SiO_4) by Solid State Reaction of MgO and SiO_2, Phil. Mag. 12, 505-14 (1965); S. L. Blank and J. A. Pask, Solubility Limits in the MgO-Fe_2O_3 System as Determined by Diffusion, J. Am. Ceram. Soc. 52, 460-61 (1969); C. Greskovich and V. S. Stubican, Interdiffusion Studies in the System MgO-Cr_2O_3, J. Phys. Chem. Solids 30 909-17 (1969), and Change of Molar Volume and Interdiffusion Coefficients in the System MgO-Cr_2O_3, J. Am. Ceram. Soc. 53, 251-53 (1970); M. Appel and J. A. Pask, Interdiffusion and Moving Boundaries in NiO-CaO and NiO-MgO Single-Crystal Couples, J. Am. Ceram. Soc. 54, 152-58 (1971); W. P. Whitney, II, and V. S. Stubican, Interdiffusion Studies in the System MgO-Al_2O_3,

J. Phys. Chem. Solids 32, 305-12 (1971); R. Dérie and L. A. Kusman, Diffusion und Reaktionen im System MgO-Fe_2O_3, Ber. Dt. Keram. Ges. 48, 381-84 (1971); and M. O'Keeffe and T. J. Ribble, Interdiffusion and the Solubility Limits of Cr_2O_3 in the Rutile Phase of TiO_2, J. Solid State Chem. 4, 351-56 (1972).

13. R. F. Davis and J. A. Pask, Diffusion and Reaction Studies in the System Al_2O_3-SiO_2, J. Am. Ceram. Soc. 55, 525-31 (1972).

14. I. A. Aksay and J. A. Pask, The Silica-Alumina System: Stable and Metastable Equilibria at 1.0 Atmosphere, Science 183, 69-71 (1974), and Stable and Metastable Equilibria in the SiO_2-Al_2O_3 System, Submitted to J. Am. Ceram. Soc.

15. N. L. Bowen and J. W. Greig, The System: Al_2O_3-SiO_2, J. Am. Ceram. Soc., 7, 238-54 and 410 (1924).

16. N. A. Toropov and F. Y. Galakhov, New Data on the System Al_2O_3-SiO_2, Dokl. Akad. Nauk SSSR 78, 299-302 (1951); N. E. Filonenko and I. V. Lavrov, On the Problem of the Behavior of Mullite at its Melting Point, Dokl. Akad. Nauk SSSR 89, 141-42 (1953); P. P. Budnikov, S. G. Tresvyatski, and V. I. Kushakovski, Making the Phase Diagram of the

System Al_2O_3-SiO_2 More Precise, Dokl. Akad. Nauk SSSR 93, 281-83 (1953); F. Y. Galakhov, Research into the Crystallisation Domain of Mullite in Alumino-Siliceous Ternary Systems, Bull. Fr. Ceram. Soc. 1958, 11-16; J. H. Welch, A New Interpretation of the Mullite Problem, Nature 186, 545-46 (1960); J. H. Welch, Observations on Composition and Melting Behaviour of Mullite, in "Transactions of the VIIth International Ceramic Congress," pp. 197-206, London (1960); H. R. Müller, The Solidification Behavior of Mullite in Bulk, Ber. Dt. Keram. Ges. 40, 316-19 (1963); N. A. Toropov and F. Y. Galakhov, The SiO_2-Al_2O_3 System, in "Eksperiment v Tekhn. Mineralog. i Petrogr., po Materialam Soveshch.," 7th, pp. 3-8, Lvov, USSR (1966); T. Horibe and S. Kuwabara, Thermo-Analytical Investigation of Phase Equilibria in the Al_2O_3-SiO_2 System, Bull. Chem. Soc. Japan 40, 972-82 (1967); and G. Rehfeld and H. E. Schwiete, Recent Results on the Melting Behavior of Mullite, Ber. Dt. Keram. Ges. 48, 258-61 (1971).

17. G. Trömel, K. -H. Obst, K. Konopicky, H. Bauer, and I. Patzak, Investigations in the SiO_2-Al_2O_3 System, Ber. Dt. Keram. Ges. 34, 397-402 (1957); K. Konopicky, Contribution to the Study of the Al_2O_3-SiO_2 System, Bull.

Fr. Ceram. Soc. 1956, 3-6; G. Trömel, in "The Physical Chemistry of Steelmaking," (J. F. Elliott, ed.) pp. 77-78, MIT Press, and John Wiley and Sons, New York (1958); and K. Konopicky, Remarks on the Equilibrium Diagram Al_2O_3-SiO_2, Ber. Dt. Keram. Ges. 40, 286 (1963).

18. S. Aramaki and R. Roy, The Mullite-Corundum Boundary in the Systems MgO-Al_2O_3-SiO_2 and CaO-Al_2O_3-SiO_2, J. Am. Ceram. Soc. 42, 644-45 (1959), Revised Equilibrium Diagram for the System Al_2O_3-SiO_2, Nature 184, 631-32 (1959), and Revised Phase Diagram for the System Al_2O_3-SiO_2, J. Am. Ceram. Soc. 45, 229-42 (1962).

19. W. H. Bauer, I. Gordon, and C. H. Moore, Flame-Fusion Synthesis of Mullite Single Crystals, J. Am. Ceram. Soc. 33, 140-43 (1950); and W. H. Bauer and I. Gordon, Flame-Fusion Synthesis of Several Types of Silicate Structures, J. Am. Ceram. Soc. 34, 250-54 (1951).

FIGURE CAPTIONS

Fig. 1. Schematic representation of diffusion structures produced by isothermal diffusion between silver and copper at two temperatures. Above the eutectic temperature (top couple at 900°C) a liquid solution layer forms between the α and β phases. The two-phase region L + α and L + β appear as interfaces. Below the eutectic, at 700°C, α and β solid solution remain in direct contact. (After F. N. Rhines[8]).

Fig. 2. The relationship between the one-phase layers formed in a Cu-Zn diffusion couple and the Cu-Zn phase diagram. The isotherm at 400°C represents the sequence of phases occurring in the diffusion couple. (After F. N. Rhines[8]).

Fig. 3. The relationship between the structure of a ternary diffusion couple and the phase diagram. Layers are developed corresponding to both one and two-phase regions lying upon the composition path between the extremes of composition; three-phase regions correspond to layer interfaces in the diffusion couple. The composition path of the diffusion couple is not usually straight as it is shown to be in this ideal example. (After F. N. Rhines[8]).

Fig. 4. The revised SiO_2-Al_2O_3 stable equilibrium phase diagram (top). The relationship between the stable phase diagram and the concentration profile of a semi-infinite SiO_2-Al_2O_3 diffusion couple is shown at temperature T below the melting point of mullite (bottom). Metastable extensions of the SiO_2-mullite system and the Al_2O_3 liquidus are superimposed on the stable SiO_2-Al_2O_3 diagram; C_A, 100% Al_2O_3; C_{ML}, concentration of Al_2O_3 in mullite at the mullite-liquid interface; C_{AM}, concentration of Al_2O_3 in mullite at the Al_2O_3 mullite interface; C_I, concentration of Al_2O_3 in liquid saturated with mullite.

Fig. 5. The microstructures of the diffusion zone between a couple of sapphire (bottom) and fused silica (top) annealed at 1903°C for 900 sec. and (A) quenched, (B) cooled at a relatively moderate rate, and (C) cooled relatively slowly. The precipitates in the top portion of the diffusion zone are (A) mullite (light gray), (B) alumina (light gray needles) and mullite (fine precipitates between the alumina needles), and (C) alumina (light gray needles). The precipitates along the interface in (B) and (C) are also alumina.

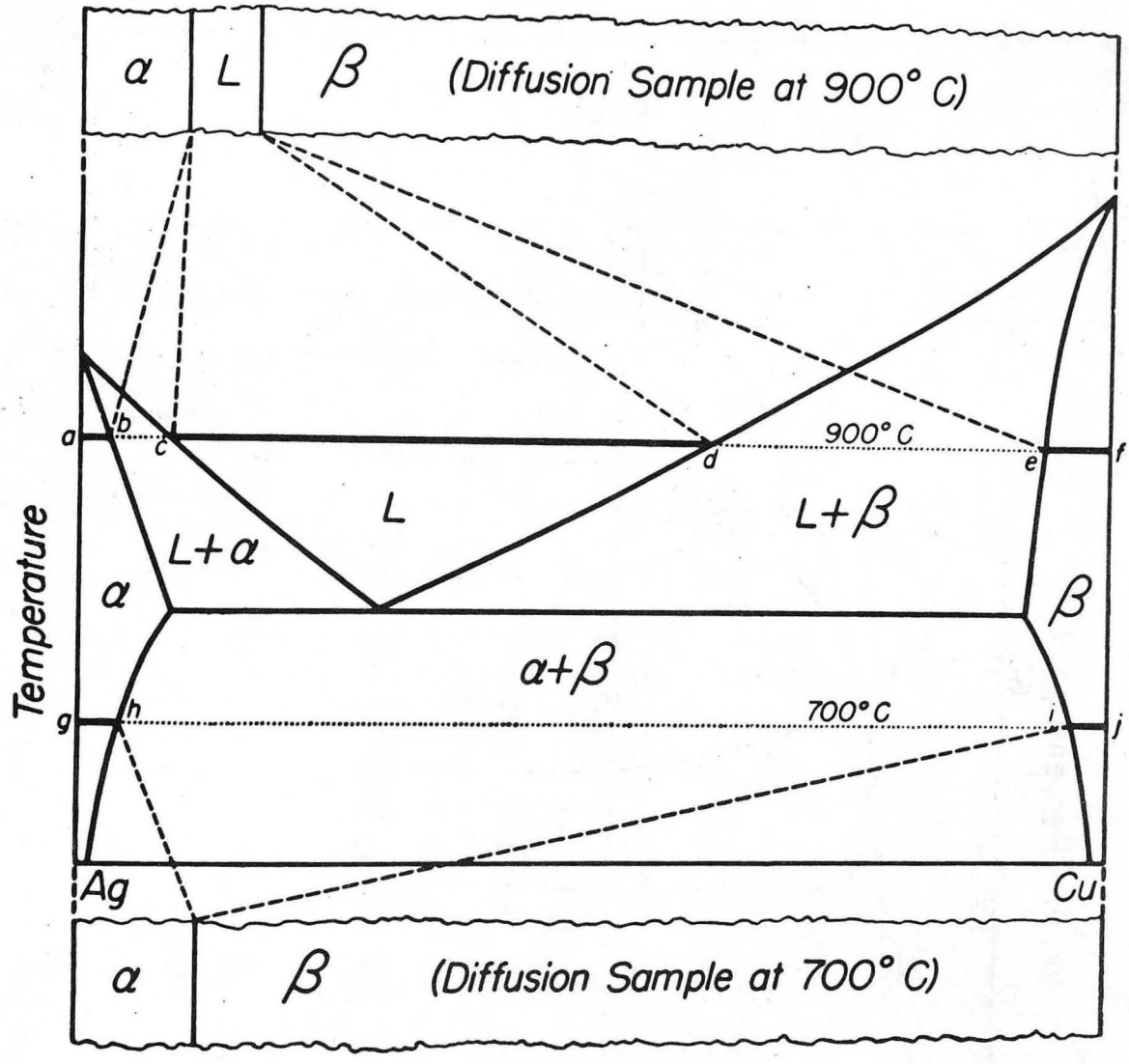

XBL 748-7059

Fig. 1

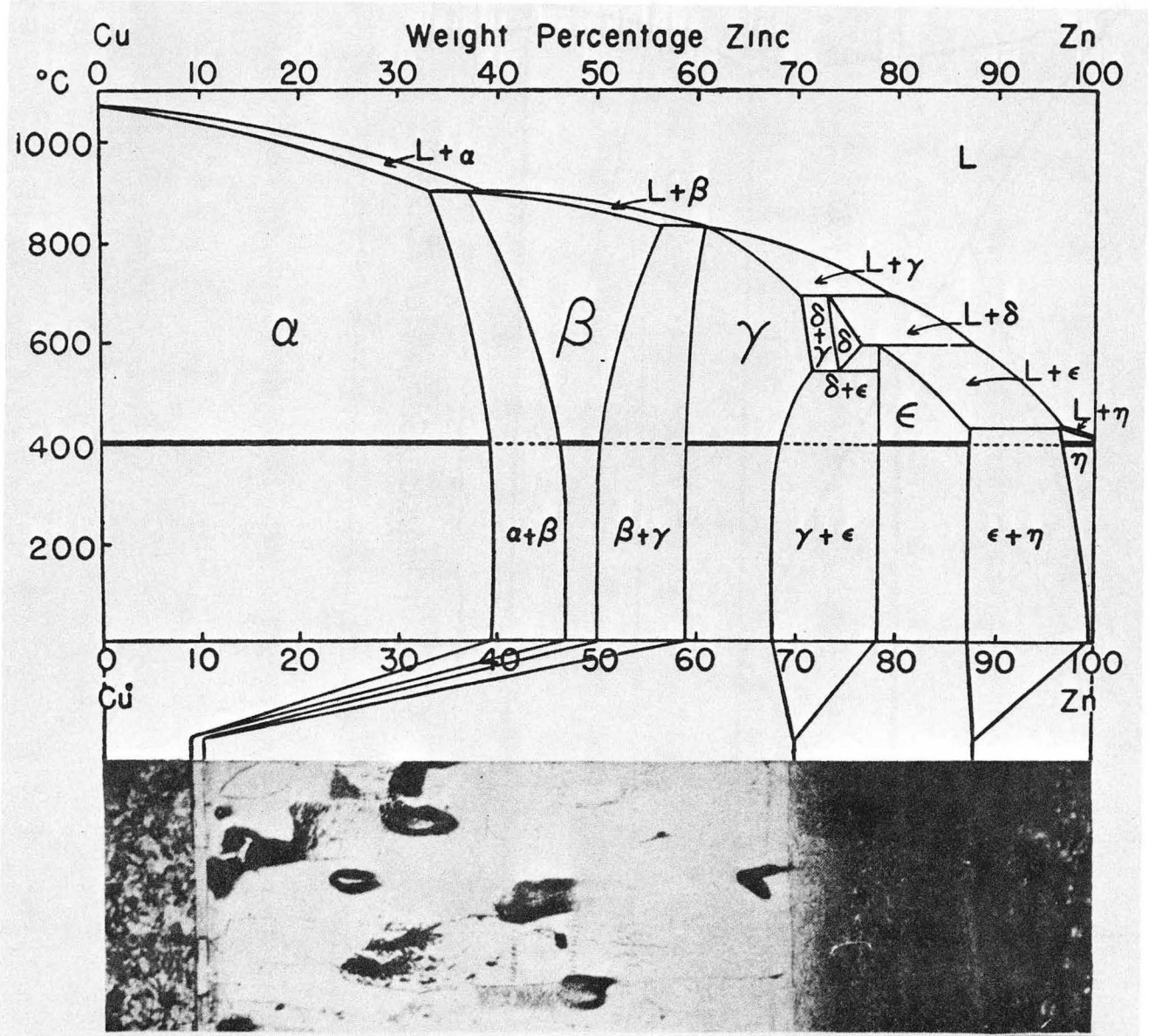

Fig. 2

XBB 748-5743

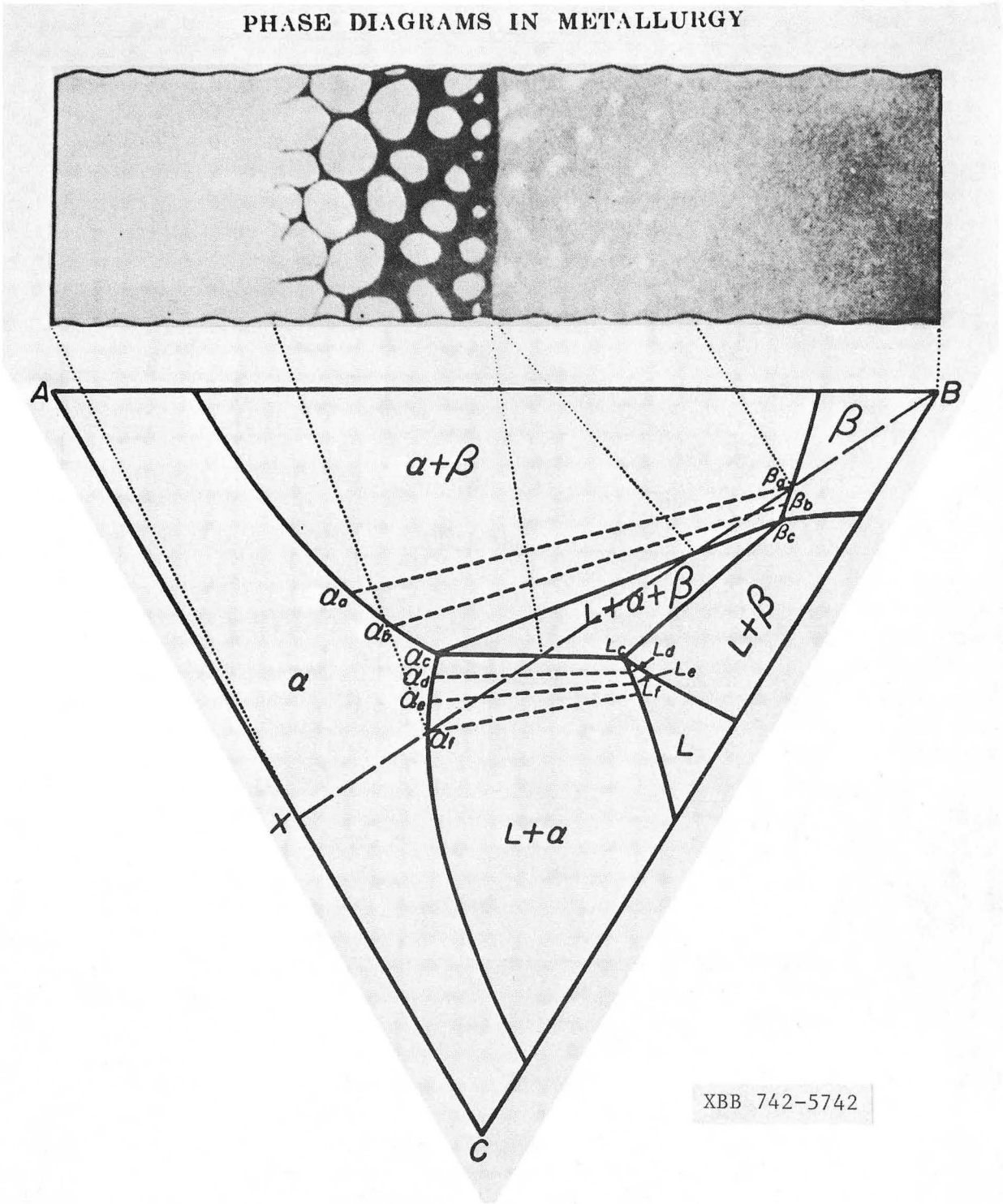
PHASE DIAGRAMS IN METALLURGY
A
B
C
α+β
β
α
L+α+β
L+β
L
L+α
X
β_a
β_b
β_c
α_o
α_b
α_c
α_d
α_e
α_f
L_c
L_d
L_e
L_f
XBB 742-5742

Fig. 3

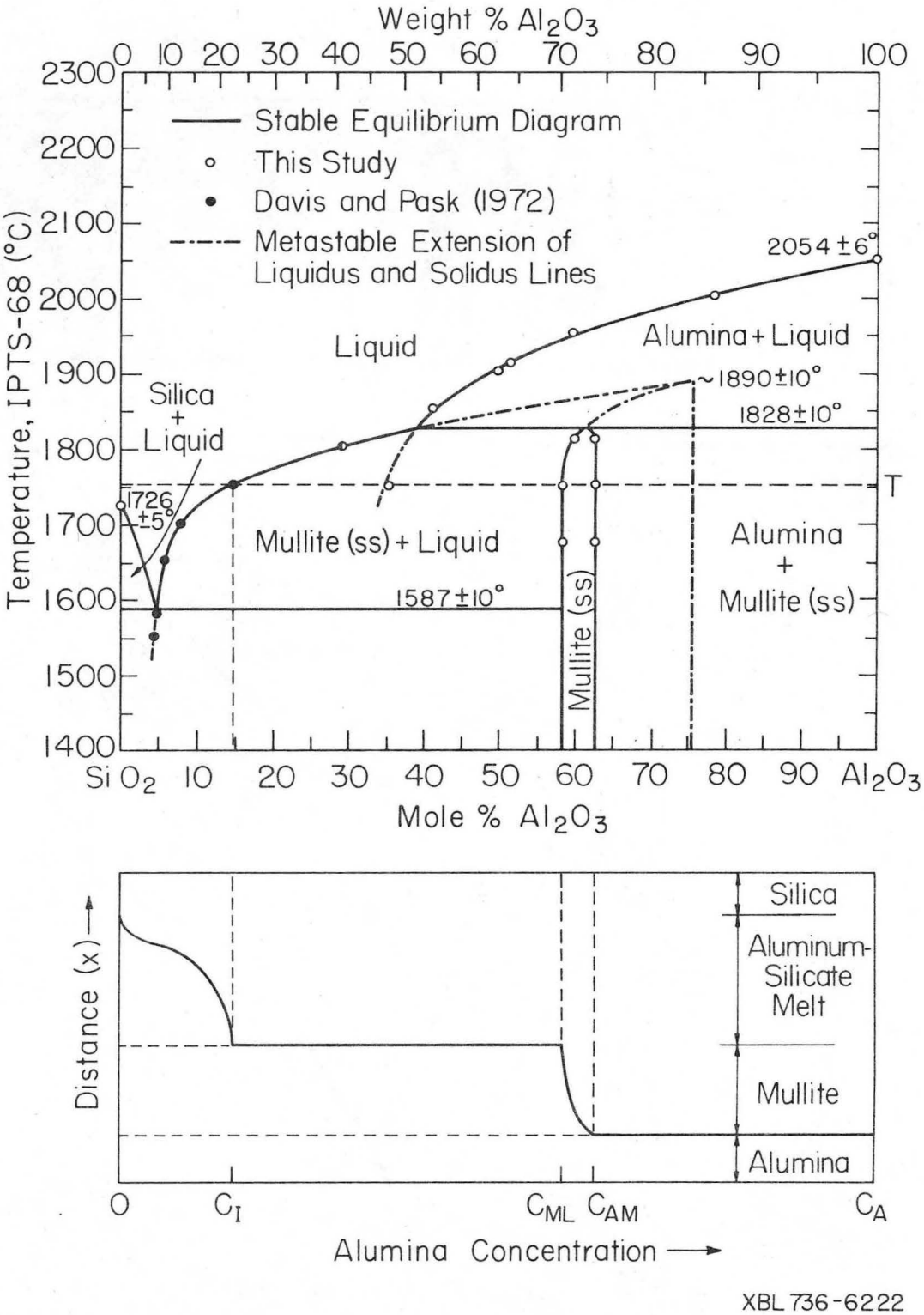
Weight % Al_2O_3
0 10 20 30 40 50 60 70 80 90 100
2300
2200
2100
2000
1900
1800
1700
1600
1500
1400
Temperature, IPTS-68 (°C)
Stable Equilibrium Diagram
This Study
Davis and Pask (1972)
Metastable Extension of Liquidus and Solidus Lines
2054 ±6°
Liquid
Alumina + Liquid
~1890±10°
1828±10°
Silica + Liquid
1726 ±5°
T
Mullite (ss) + Liquid
1587±10°
Mullite (ss)
Alumina + Mullite (ss)
SiO_2 10 20 30 40 50 60 70 80 90 Al_2O_3
Mole % Al_2O_3
Distance (x) →
Silica
Aluminum-Silicate Melt
Mullite
Alumina
0
C_I
C_{ML}
C_{AM}
C_A
Alumina Concentration →
XBL 736-6222

Fig. 4

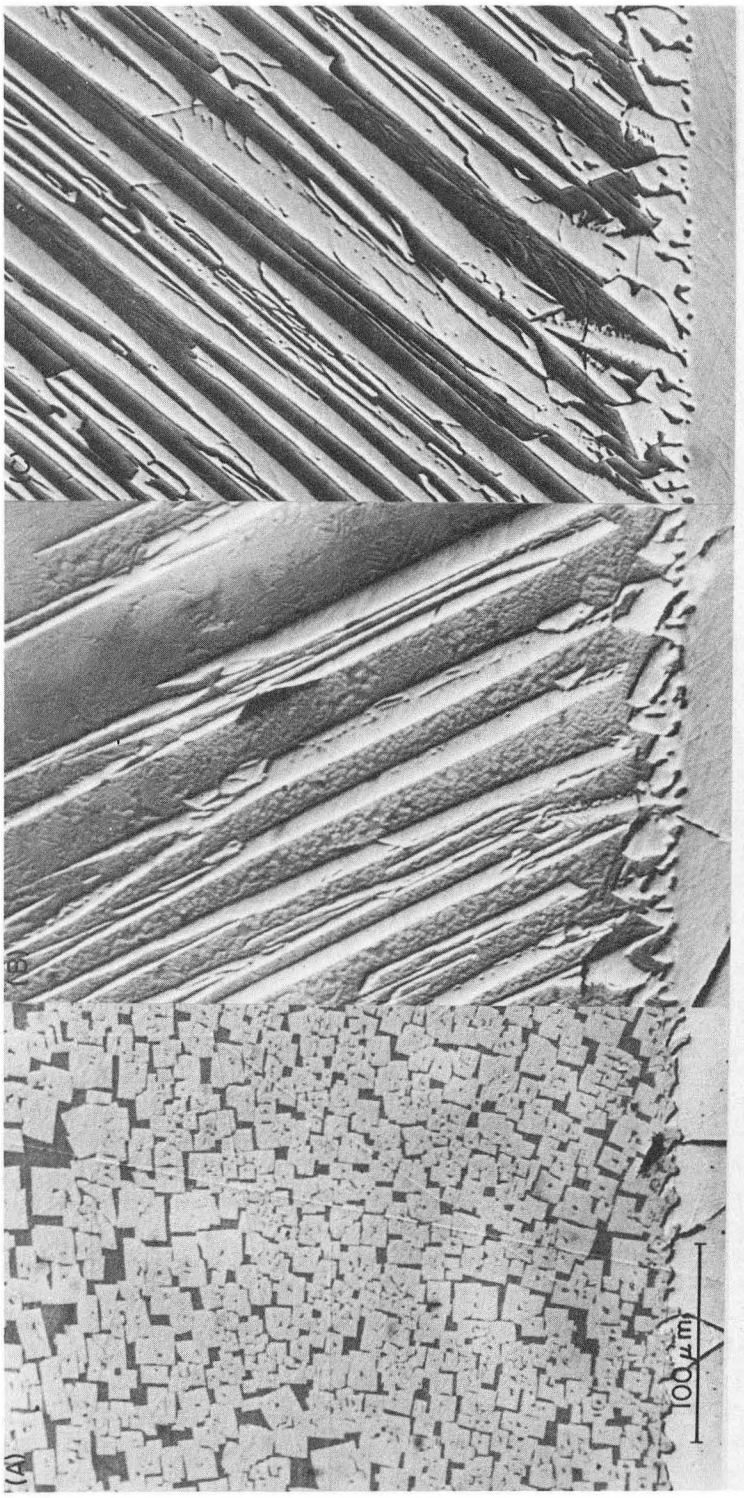

XBB 7210-5192

Fig.5

TECHNICAL INFORMATION DIVISION
LAWRENCE BERKELEY LABORATORY
UNIVERSITY OF CALIFORNIA
BERKELEY, CALIFORNIA 94720